Inorg. Chem. **2005**, *44*, 3473–3478

Aerobic Catechol Oxidation Catalyzed by a Bis(μ-oxo)dimanganese(III,III) Complex via a Manganese(II)–Semiquinonate Complex

Yutaka Hitomi,*,† Akira Ando,† Hajime Matsui,† Tomoyuki Ito,† Tsunehiro Tanaka,† Seiji Ogo,‡ and Takuzo Funabiki*,§

Department of Molecular Engineering, Graduate School of Engineering, Kyoto University, Katsura, Nishikyo-ku, Kyoto 615-8510, Japan, Department of Material and Life Science, Graduate School of Engineering, Osaka University, Suita, Osaka 565-0871, Japan, and Biomimetics Research Center, Doshisha University, Kyo-Tanabe, Kyoto 610-0321, Japan

Received January 24, 2005

A 3,5-di-*tert*-butyl-1,2-semiquinonato (DTBSQ) adduct of Mn(II) was prepared by a reaction between $Mn^{II}(TPA)Cl_2$ (TPA = tris(pyridin-2-ylmethyl)amine) and DTBSQ anion and was isolated as a tetraphenylborate salt. The X-ray crystal structure revealed that the complex is formulated as a manganese(II)–semiquinonate complex $[Mn^{II}(TPA)(DTBSQ)]^+$ (**1**). The electronic spectra in solution also indicated the semiquinonate coordination to Mn. The exposure of **1** in acetonitrile to dioxygen afforded 3,5-di-*tert*-butyl-1,2-benzoquione and a bis(μ-oxo)dimanganese(III,III) complex $[Mn^{III}_2(\mu\text{-oxo})_2(TPA)_2]^{2+}$ (**2**). The reaction of **2** with 3,5-di-*tert*-butylcatechol ($DTBCH_2$) quantitatively afforded two equivalents of **1** under anaerobic conditions. The highly efficient catalytic oxidation of $DTBCH_2$ with dioxygen was achieved by combining the above two reactions, that is, by constructing a catalytic cycle involving both manganese complexes **1** and **2**. It was revealed that dioxygen is reduced to water but not to hydrogen peroxide in the catalytic cycle.

Introduction

The reactivity of metal−catecholate complexes with dioxygen has attracted intense attention in the field of bioinorganic chemistry because catechol oxidation and oxygenation catalyzed by metalloenzymes are known to play important roles in biological systems.[1−5] Catechol dioxygenases contain a mononuclear iron or manganese active center to perform the oxygenative cleavage of aromatic rings of catechols, while catechol oxidases have a dinuclear copper active center to catalyze the aerobic oxidation of catechol derivatives to the corresponding *o*-quinones. Although the two enzymes perform distinct reactions, both enzymes form a metal−catecholate complex as a reaction intermediate in the catalytic cycles. To explore the mechanisms of the reactions performed by these enzymes, various types of catecholate complexes have been developed with iron or copper, and their reactivities with dioxygen have been studied.[2−4,6−22] In addition, catecholate complexes with other

* Author to whom correspondence should be addressed. E-mail: hitomi@moleng.kyoto-u.ac.jp.

† Kyoto University.

‡ Osaka University.

§ Doshisha University.

(1) Funabiki, T. *Oxygenases and Model Systems, Catalysis by Metal Complexes*; Kluwer: Dordrecht, The Netherlands, 1997; Vol. 19.
(2) Costas, M.; Mehn, M. P.; Jensen, M. P.; Que, L., Jr. *Chem. Rev.* **2004**, *104*, 939.
(3) Lewis, E. A.; Tolman, W. B. *Chem. Rev.* **2004**, *104*, 1047.
(4) Than, R.; Feldmann, A. A.; Krebs, B. *Coord. Chem. Rev.* **1999**, *182*, 211−241.
(5) Gerdemann, C.; Eicken, C.; Krebs, B. *Acc. Chem. Res.* **2002**, *35*, 183−191.
(6) Yamahara, R.; Ogo, S.; Masuda, H.; Watanabe, Y. *J. Inorg. Biochem.* **2002**, *88*, 284−294.
(7) Kodera, M.; Kawata, T.; Kano, K.; Tachi, Y.; Itoh, S.; Kojo, S. *Bull. Chem. Soc. Jpn.* **2003**, *76*, 1957−1964.
(8) Selmeczi, K.; Reglier, M.; Giorgi, M.; Speier, G. *Coord. Chem. Rev.* **2003**, *245*, 191−201.
(9) Ackermann, J.; Meyer, F.; Kaifer, E.; Pritzkow, H. *Chem.−Eur. J.* **2002**, *8*, 247−258.
(10) Belle, C.; Beguin, C.; Gautier-Luneau, I.; Hamman, S.; Philouze, C.; Pierre, J. L.; Thomas, F.; Torelli, S.; Saint-Aman, E.; Bonin, M. *Inorg. Chem.* **2002**, *41*, 479−491.
(11) Neves, A.; Rossi, L. M.; Bortoluzzi, A. J.; Szpoganicz, B.; Wiezbicki, C.; Schwingel, E. *Inorg. Chem.* **2002**, *41*, 1788−1794.
(12) Kaizer, J.; Pap, J.; Speier, G.; Parkanyi, L.; Korecz, L.; Rockenbaur, A. *J. Inorg. Biochem.* **2002**, *91*, 190.
(13) Speier, G.; Tyeklar, Z.; Toth, P.; Speier, E.; Tisza, S.; Rockenbauer, A.; Whalen, A. M.; Alkire, N.; Pierpont, C. G. *Inorg. Chem.* **2001**, *40*, 5653−5659.
(14) Torelli, S.; Belle, C.; Gautier-Luneau, I.; Pierre, J. L.; Saint-Aman, E.; Latour, J. M.; Le Pape, L.; Luneau, D. *Inorg. Chem.* **2000**, *39*, 3526−3536.
(15) Berreau, L. M.; Mahapatra, S.; Halfen, J. A.; Houser, R. P.; Young, J., V. G.; Tolman, W. B. *Angew. Chem., Int. Ed.* **1999**, *38*, 207.

10.1021/ic050109d CCC: $30.25
Published on Web 04/08/2005

metal ions, such as manganese, cobalt, rhodium, and iridium, have also provided valuable information on the reaction mechanisms.[23−34]

In the reaction mechanism of the iron(III)-containing catechol dioxygenase, the iron(II)−semiquinonate (Fe(II)−SQ) state is considered to be responsible for the oxygenation reaction of the iron(III)−catecholate (Fe(III)−Cat) complex with dioxygen.[2,35−37] In relevance to this mechanism, we have reported preliminary results on the formation and oxygen reactivity of a Mn(II)−SQ complex.[38] Caneschi and Dei reported a valence tautomerism between Mn(II)−SQ and Mn(III)−Cat species in a mononuclear manganese complex $[Mn(cth)(diox)]^+$ (cth = 5,7,7,12,14,14-hexamethyl-1,4,8,11-tetrazacyclotetradecane, diox = dioxolane ligand).[39] As for the reactivity of these two species with dioxygen, in the footnote they briefly mentioned the remarkable distinction between the Mn(III)−DTBC (DTBC = 3,5-di-*tert*-butylcatecholate) and Mn(II)−DTBSQ (DTBSQ = 3,5-di-*tert*-butyl-1,2-semiquinonate) species; the Mn(III)−DTBC is stable for days, while the Mn(II)−DTBSQ affords oxo-dimers of the manganese complex as well as 3,5-di-*tert*-butyl-*o*-benzoquinone (DTBQ) and the extradiol cleaving products, 3,5-bis-(1,2-dimethylethyl)- and 4,6-bis(1,1-dimethylethyl)-2H-pyranones. Because no reaction mechanism has been proposed for both reactions, we here studied in detail the oxidation process of the Mn(II)−DTBSQ species to DTBQ and its role as an intermediate in a catalytic catechol oxidation.

Scheme 1. Catalytic Cycle of the Aerobic Oxidation of $DTBCH_2$

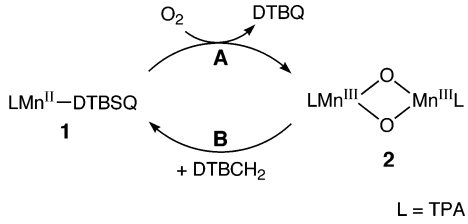

As a Mn(II)−SQ species, we synthesized $[Mn^{II}(TPA)(DTBSQ)]^+$ (TPA = tris(pyridin-2-ylmethyl)amine) (**1**). The addition of O_2 to **1** in acetonitrile did not afford any cleavage products of the DTBSQ ligand but yielded DTBQ and a novel bis(μ-oxo)dimanganese(III,III) complex $[Mn^{III}_2(\mu\text{-}oxo)_2(TPA)_2]^{2+}$ (**2**) as shown by path A in Scheme 1. In addition, **2** was found to react with 3,5-di-*tert*-butylcatechol ($DTBCH_2$) to give two equivalents of **1** as shown by path B in Scheme 1. These two reactions achieved an efficient catalytic aerobic oxidation of $DTBCH_2$ to DTBQ by manganese complexes as shown in Scheme 1.

Experimental Section

General Procedures. The ligand TPA and sodium salt of DTBSQ anion (NaDTBSQ) were prepared according to published procedures.[40,41] All other reagents were purchased from commercial sources and used as received. Air-sensitive manipulations, including the synthesis of **1**, were performed under nitrogen in an MBraun glovebox.

$Mn^{II}(TPA)Cl_2$. To a solution of $MnCl_2\cdot 6H_2O$ (3.17 g, 16.0 mmol) in MeOH (40 mL), a solution of TPA (4.64 g, 16.0 mmol) in MeOH (40 mL) was added at 50 °C. The resulting solution was stirred for 60 min and cooled to room temperature. Evaporation of the solvent produced white precipitates. Recrystallization from MeOH yielded white crystals. Yields: 8.12 g (51%). Anal. Calcd for $C_{18}H_{18}Cl_2MnN_4$: C, 51.90; H, 4.36; N, 13.5; Cl, 17.0. Found: C, 51.96; H, 4.14; N, 13.50; Cl, 17.14.

$[Mn^{II}(TPA)(DTBSQ)]BPh_4$ (1). Equimolar amounts of $Mn^{II}(TPA)Cl_2$ (83 mg, 0.20 mmol) and NaDTBSQ (49 mg, 0.20 mmol) were dissolved in 80 mL of EtOH, resulting in a green solution. After adding 2.0 mL of EtOH containing $NaBPh_4$ (68 mg, 0.20 mmol), the green solution was allowed to stand overnight at −30 °C to produce a green solid. Recrystallization from acetonitrile yielded large green crystals. Yields: 79 mg (45%). ESI-MS: *m*/*z*: 565.5 $[M-BPh_4]^+$. Anal. Calcd for $C_{56}H_{58}BMnN_4O_2\cdot CH_3CN$: C, 75.24; H, 6.64; N, 7.56. Found: C, 74.96; H, 6.55; N, 7.65.

$[Mn^{III}_2(\mu\text{-}oxo)_2(TPA)_2](BPh_4)_2$ (2). A solution of **1** in acetonitrile (20 mM) was allowed to stand overnight under air. The green solution turned to yellow, and brown crystals were precipitated suitable for X-ray diffraction analysis. ESI-MS: *m*/*z*: 1041.5 $[M-BPh_4]^+$, 361.3 $[M-2BPh_4]^{2+}$. Anal. Calcd for $C_{84}H_{76}B_2Mn_2N_8O_2$: C, 74.13; H, 5.63; N, 8.23. Found: C, 74.08; H, 5.61; N, 8.25.

Physical Measurements. ^1H NMR spectra were recorded on a JEOL AL300 FT-NMR spectrometer. UV−vis spectra were recorded on an Otsuka Electronics photodiode array spectrometer

(16) Monzani, E.; Battaini, G.; Perotti, A.; Casella, L.; Gullotti, M.; Santagostini, L.; Nardin, G.; Randaccio, L.; Geremia, S.; Zanello, P.; Opromolla, G. *Inorg. Chem.* **1999**, *38*, 5359−5369.
(17) Monzani, E.; Quinti, L.; Perotti, A.; Casella, L.; Gullotti, M.; Randaccio, L.; Geremia, S.; Nardin, G.; Faleschini, P.; Tabbi, G. *Inorg. Chem.* **1998**, *37*, 553−562.
(18) Malachowski, M. R.; Huynh, H. B.; Tomlinson, L. J.; Kelly, R. S.; Furbee, J. W. *J. Chem. Soc., Dalton Trans.* **1995**, 31−36.
(19) Balla, J.; Kiss, T.; Jameson, R. F. *Inorg. Chem.* **1992**, *31*, 58−62.
(20) Chyn, J. P.; Urbach, F. L. *Inorg. Chim. Acta* **1991**, *189*, 157−163.
(21) Speier, G. *J. Mol. Catal.* **1986**, *37*, 259−267.
(22) Oishi, N.; Nishida, Y.; Ida, K.; Kida, S. *Bull. Chem. Soc. Jpn* **1980**, *53*, 2847−2850.
(23) Reynolds, M. F.; Costas, M.; Ito, M.; Jo, D. H.; Tipton, A. A.; Whiting, A. K.; Que, L., Jr. *J. Biol. Inorg. Chem.* **2003**, *8*, 263−272.
(24) Triller, M. U.; Pursche, D.; Hsieh, W. Y.; Pecoraro, V. L.; Rompel, A.; Krebs, B. *Inorg. Chem.* **2003**, *42*, 6274−6283.
(25) Shaikh, N.; Panja, A.; Banerjee, P.; Ali, M. *Transiton Met. Chem.* **2003**, *28*, 871−880.
(26) Reddig, N.; Pursche, D.; Krebs, B.; Rompel, A. *Inorg. Chim. Acta* **2004**, *357*, 2703−2712.
(27) Simandi, L. I.; Simandi, T. M.; May, Z.; Besenyei, G. *Coord. Chem. Rev.* **2003**, *245*, 85−93.
(28) Bencini, A.; Bill, E.; Scozzafava, A.; Totti, F. *Chem.−Eur. J.* **2003**, *9*, 3015−3023.
(29) Bencini, A.; Bill, E.; Mariotti, F.; Totti, F.; Scozzafava, A.; Vargas, A. *Inorg. Chem.* **2000**, *39*, 1418.
(30) Hartl, F.; Barbaro, P.; Bell, I. M.; Clark, R. J. H.; Snoeck, T. L.; Vlcek, A. *Inorg. Chim. Acta* **1996**, *252*, 157.
(31) Barbaro, P.; Bianchini, C.; Linn, K.; Mealli, C.; Meli, A.; Vizza, F.; Laschi, F.; Zanello, P. *Inorg. Chim. Acta* **1992**, *200*, 31.
(32) Barbaro, P.; Bianchini, C.; Frediani, P.; Meli, A.; Vizza, F. *Inorg. Chem.* **1992**, *31*, 1523.
(33) Barbaro, P.; Bianchini, C.; Mealli, C.; Meli, A. *J. Am. Chem. Soc.* **1991**, *113*, 3181.
(34) Bianchini, C.; Frediani, P.; Laschi, F.; Meli, A.; Vizza, F.; Zanello, P. *Inorg. Chem.* **1990**, *29*, 3402.
(35) Cox, D. D.; L, Q., Jr. *J. Am. Chem. Soc.* **1988**, *110*, 8085−8092.
(36) Funabiki, T.; Yamazaki, T. *J. Mol. Catal., A-Chem.* **1999**, *150*, 37−47.
(37) Hitomi, Y.; Yoshida, M.; Higuchi, M.; Minami, H.; Tanaka, T.; Funabiki, T. *J. Inorg. Biochem.* **2005**, *99*, 755−763.
(38) Funabiki, T.; Ito, T.; Matsui, H.; Fukui, A.; Aki, M.; Ogo, S.; Watanabe, Y. *J. Inorg. Biochem.* **1999**, *74*, 133.
(39) Caneschi, A.; Dei, A. *Angew. Chem., Int. Ed.* **1998**, *37*, 3005.
(40) Tyeklar, Z.; Jacobson, R. R.; Wei, N.; Murthy, N. N.; Zubieta, J.; Karlin, K. D. *J. Am. Chem. Soc.* **1993**, *115*, 2677.
(41) White, L. S.; Hellman, E. J.; Que, L., Jr. *J. Org. Chem.* **1982**, *47*, 3766.

Table 1. Crystal Data for Complexes **1** and **2**

	1	**2**
formula	$C_{58}H_{61}BN_5MnO_2$	$C_{84}H_{76}B_2N_8Mn_2O_2$
formula weight	925.90	1361.07
color	green	brown
crystal system	triclinic	monoclinic
space group	*P*1 (no. 2)	*C*2/*c* (no. 15)
T (K)	223	243
a (Å)	13.236(2)	19.474(2)
b (Å)	13.659(2)	14.884(2)
c (Å)	14.778(2)	24.538(3)
α (deg)	94.841(3)	
β (deg)	101.952(4)	105.370(3)
γ (deg)	97.012(4)	
V (Å^3)	2577.7(7)	6858.3(1)
Z	2	4
D_{calc} (g cm^{-3})	1.193	1.318
radiation	Mo Kα ($\lambda = 0.71070$ Å)	Mo Kα ($\lambda = 0.71070$ Å)
μ (mm^{-1})	0.302	0.425
no. of reflctns measd	11438	7748
no. of observations	8632	4372
no. of variables	604	442
R^a ($I > 2.00s(I)$)	0.055	0.066
$R_w{}^a$ ($I > 2.00s(I)$)	0.128	0.180
GOF	1.618	1.055

[a] $R = \Sigma(|F_o| - |F_c|)/\Sigma|F_o|$; $R_w = [\Sigma(w|F_o| - |F_c|)^2/\Sigma w|F_o|^2]^{1/2}$; $w = 1/\sigma^2(F_o)$.

MCPD-2000 with an Otsuka Electronics optical fiber attachment or a Hewlett-Packard 8453 photodiode array spectrophotometer equipped with a Unisoku thermostated cell holder designed for low-temperature measurements. For the former apparatus, the temperature was controlled with a Komatsu−Yamato bath circulator. Electrospray ionization mass spectrometry (ESI-MS) spectra were obtained on an Applied Biosystems PE-Sciex API2000 mass spectrometer. Elemental analyses were performed by the Microanalytical Center of Kyoto University.

Kinetics and Product Analysis. A solution was prepared by dissolving **1** (0.01 mmol) in anhydrous acetonitrile (2 mL) under N_2 in a glovebox. Oxidation was started by adding the solution of **1** by syringe into the solution equilibrated with 1 atm of O_2 at 298 K. Reaction rate constants were determined by monitoring a decrease of the absorption at 750 nm because of the DTBSQ complex. After the reaction was completed, 5 mM solution of anthracene in CH_2Cl_2 (0.1 mL) was added to the solution as an internal standard for the quantitative analysis and then was evaporated. Identification and quantification of the oxidized products were carried out by ^{1}H NMR and ESI-MS spectroscopies.

X-ray Structure Determination. The crystals were mounted on a glass capillary. Data collection was performed on a Rigaku CCD diffractometer (Mo Kα, $\lambda = 0.71070$ Å) and processed with Crystal Clear. The structures were solved using direct methods and refined with full-matrix least squares. All non-hydrogen atoms and hydrogen atoms were refined anisotropically and isotropically, respectively. All hydrogen atoms were located at the calculated positions, and they were assigned a fixed displacement and constrained to ideal geometry. All calculations were performed by using the teXsan crystallographic software program package. Summaries of the fundamental crystal data and experimental parameters for the structure determination of complexes **1** and **2** are given in Table 1.

Results and Discussion

Preparation and Characterization of 1. The reaction of $Mn^{II}(TPA)Cl_2$ with NaDTBSQ in EtOH under N_2 yielded the green product $[Mn(TPA)(diox)]^+$. The cation was precipitated as a tetraphenylborate salt (**1**). Single crystals suitable for X-ray diffraction analysis were obtained as green crystals from an acetonitrile solution of **1**. A thermal ellipsoid plot of the crystal structure of the cation is shown in Figure 1. Selected bond lengths and angles are listed in Table 2. The Mn center is coordinated by N_4O_2 atoms, that is, four nitrogen atoms from TPA and two oxygen atoms from the bidentate semiquinonate ligand. The coordination geometry around the manganese is highly distorted octahedral. The Mn−N bond length is significantly longer for the aliphatic nitrogen atom (2.334 Å) than for the pyridine nitrogen atoms (2.237−2.253 Å). The O(1)−Mn(1)−O(2) angle of 76.0° is comparable to that of a previously reported Mn(II)−SQ complex.[42] The C−O and C(1)−C(2) bond lengths are typical of SQ ligands.[43] Thus, the structural parameters indicate the formulation of the cation as $[Mn^{II}(TPA)(DTBSQ)]^+$.

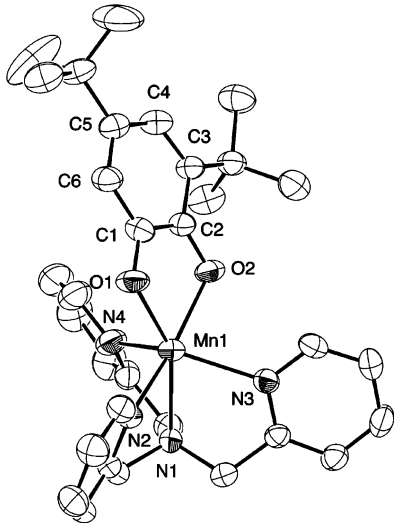

Figure 1. ORTEP drawing of $[Mn^{II}(TPA)(DTBSQ)]^+$. 50% probability ellipsoids are shown.

Table 2. Selected Bond Distances and Angles for Complex **1**

	bond distances (Å)		
Mn−O(1)	2.121(2)	Mn−O(2)	2.138(2)
Mn−N(1)	2.334(2)	Mn−N(2)	2.237(2)
Mn−N(3)	2.243(2)	Mn−N(4)	2.253(3)
C(1)−O(1)	1.282(3)	C(1)−O(2)	1.278(3)
C(1)−C(2)	1.428(4)		
	bond angles (deg)		
O(1)−Mn−O(2)	74.86(6)	N(1)−Mn−N(2)	71.84(7)
N(1)−Mn−N(3)	73.60(7)	N(1)−Mn−N(4)	70.95(7)

The UV−vis spectrum of **1** in acetonitrile showed an intense band at around 750 nm with a vibronic progression, which is diagnostic of an SQ ligand (Figure 2).[44] The spectral features are virtually identical to those reported for the $[Mn^{II}(cth)(DTBSQ)]^+$ species in acetone.[39] It was reported that the $[Mn(cth)(diox)]^+$ complex exhibits valence tautomerization from Mn(II)−SQ to Mn(III)−Cat forms in the solid state as the temperature is lowered, where the latter species is yellow and does not show the intense band at around 750

(42) Attia, A. S.; Jung, O.-S.; Pierpont, C. G. *Inorg. Chim. Acta* **1994**, *226*, 91.
(43) Pierpont, C. G.; Lange, C. W. *Prog. Coord. Chem.* **1993**, *41*, 381.
(44) Benlli, C.; Dei, A.; Gatteschi, D.; Pardi, L. *Inorg. Chem.* **1989**, *28*, 1476.

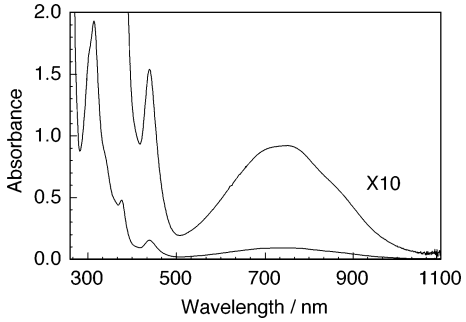

Figure 2. Electronic absorption spectrum of $[Mn^{II}(TPA)(DTBSQ)]BPh_4$ in acetonitrile (0.2 mM) at 298 K.

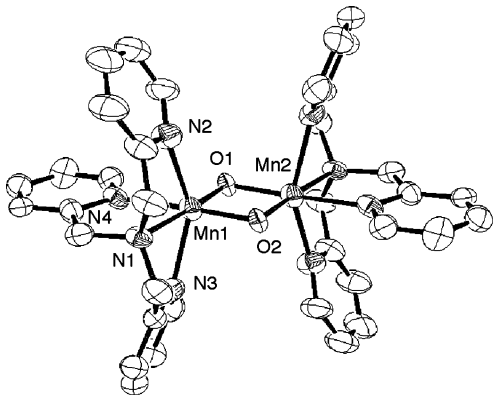

Figure 3. ORTEP drawing of $[Mn^{III}_2(\mu\text{-oxo})_2(TPA)_2]^{2+}$. 50% probability ellipsoids are shown.

nm.[39] Even when the temperature was lowered from 298 to 213 K, the solution of **1** retained the spectral features characteristic of an SQ ligand and only the vibronic progression of ca. 1460 cm^{-1} became clearer (Figure S1). These results indicate that **1** retains the Mn(II)−SQ form in solution in the temperature range from 213 to 298 K.

Reaction of 1 with Dioxygen. Upon exposure to O_2, the acetonitrile solution of **1** immediately changed color from green to yellow. The electronic absorption spectrum of the product solution showed an intense absorption at 400 nm and a weak shoulder peak at around 550 nm, which indicates the production of DTBQ. The NMR spectrum of the product revealed that the DTBSQ ligand was exclusively oxidized to DTBQ. The solution after oxidation was also analyzed by ESI-MS. Major peaks were observed at 361.3 and 1041.5 *m*/*z*, which can be attributed to $[Mn^{III}_2(\mu\text{-oxo})_2(TPA)_2]^{2+}$ and $[Mn^{III}_2(\mu\text{-oxo})_2(TPA)_2]BPh_4^+$, respectively. Prolonged standing of the solution afforded suitable crystals for a single-crystal X-ray structure analysis. A view of the cation is given in Figure 3. Principal distances and angles are listed in Table 3. The cation has an inversion center, and the two bridging oxo atoms bind to the manganese atoms unsymmetrically. Each manganese center adopts a distorted octahedral environment. The Mn−Mn separation is 2.656 (2) Å, which is slightly longer than the value of 2.643(1) Å reported for the one-electron oxidized form $[Mn^{III}Mn^{IV}(\mu\text{-oxo})_2(TPA)_2]^{3+}$.[45] The Mn1−N2 and Mn1−N3 bond lengths are ca. 0.24 Å longer than the Mn1−N4, suggestive of Jahn−Teller distorted high-spin Mn(III) centers. The UV−vis spectrum of **2** exhibited a weak broad absorption at around 500 nm, which can be attributed to the d−d band of the Mn(III) site (Figure S2). These spectral features are comparable to those reported for several bis(μ-oxo)dimanganese(III,III) complexes.[46]

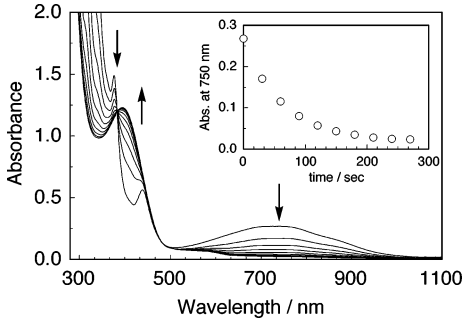

Figure 4. Progress of the reaction of **1** with dioxygen in acetonitrile at 273 K as monitored by electronic absorption spectroscopy. The spectra are shown at 30-s intervals. Inset: time course of absorbance changes at 750 nm.

Table 3. Selected Bond Distances and Angles for Complex **2**

bond distances (Å)			
Mn(1)−Mn(2)	2.656(2)	Mn(1)−O(1)	1.866(3)
Mn(1)−O(2)	1.861(3)	Mn(1)−N(1)	2.166(4)
Mn(1)−N(2)	2.328(5)	Mn(1)−N(3)	2.308(5)
Mn(1)−N(4)	2.079(4)		
bond angles (deg)			
O(1)−Mn(1)−O(2)	89.1(1)	Mn(1)−O(1)−Mn(2)	90.9(1)
N(1)−Mn(1)−N(2)	74.6(2)	N(1)−Mn(1)−N(3)	73.7(2)
N(1)−Mn(1)−N(4)	80.4(2)		

The oxidation reaction was monitored by UV−vis spectroscopy. Figure 4 shows the electronic absorption spectral changes of the reaction progress under 1 atm of O_2 at 273 K. Here, the absorptions at 377 and 750 nm are diminished and an intense absorption at 400 nm increases, accompanied by an isosbestic point at 384 nm. Even at 213 K, the oxidation reaction caused the similar spectral changes, indicating the absence of detectable reaction intermediates. These results suggest that the formation of **2** is much faster than the oxidation of **1**. The oxidation rate constant at 298 K was estimated to be 19.9 ± 0.6 M^{-1} s^{-1} by fitting the decay at 750 nm to a single-exponential function, which is comparable to the value of 18 M^{-1} s^{-1} for $[Fe^{III}(TPA)(DTBC)]BPh_4$ under the same conditions.[37,47]

Reaction of 2 with $DTBCH_2$. Upon addition of $DTBCH_2$ to an acetonitrile solution of **2** under anaerobic conditions, the absorptions at 435 and 750 nm increased almost linearly until two equivalents of $DTBCH_2$ to **2** were added (Figure 5). The reaction product was identified as $[Mn^{II}(TPA)(DTBSQ)]^+$ on the basis of a spectroscopic comparison with **1** and by ESI-MS. The spectral changes indicate the quantitative formation of $[Mn^{II}(TPA)(DTBSQ)]^+$ from **2**. The formation of $[Mn^{II}(TPA)(DTBSQ)]^+$ by the reaction of **2** with $DTBCH_2$ is accounted for by the formation of $[Mn^{III}(TPA)(DTBC)]^+$ and its conversion to $[Mn^{II}(TPA)(DTBSQ)]^+$ by valence tautomerization. A similar reaction was reported with

(45) Towle, D. K.; Botsford, C. A.; Hodgson, D. J. *Inorg. Chim. Acta* **1988**, *141*, 167.

(46) Goodson, P. A.; Oki, A. R.; Glerup, J.; Hodgson, D. J. *J. Am. Chem. Soc.* **1990**, *112*, 6248.

(47) Jang, H. G.; Cox, D. D.; Que, L. *J. Am. Chem. Soc.* **1991**, *113*, 9200−9204.

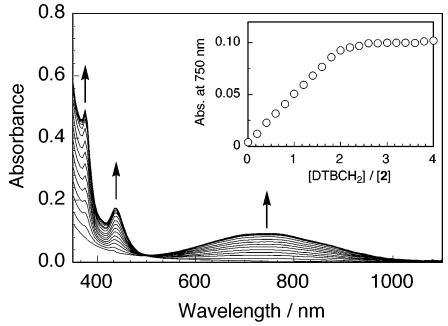

Figure 5. Spectrophotometric titration of **2** with $DTBCH_2$ in acetonitrile at 298 K under N_2. The arrows indicate changes due to increasing concentration of $DTBCH_2$. [**2**] = 0.1 mM. [$DTBCH_2$] = 0−0.4 mM. Inset: absorbance at 750 nm plotted versus equivalents of $DTBCH_2$ added.

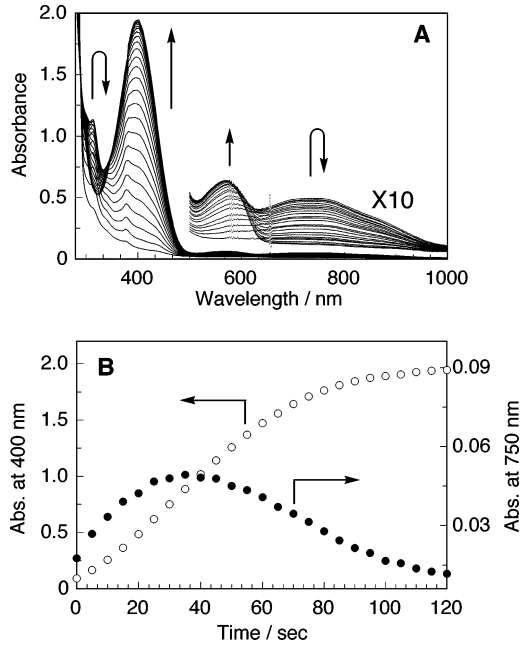

Figure 6. Aerobic oxidation of $DTBCH_2$ to DTBQ in the presence of **2** in acetonitrile at 298 K under 1 atm O_2 monitored by electronic absorption spectroscopy. (B) Plots of absorbance at 400 and 750 nm vs time. Conditions: [**2**] = 0.1 mM, [$DTBCH_2$] = 1.0 mM.

copper complexes, that is, the reaction of a bis(μ-oxo)-dicopper(III,III) complex with $DTBCH_2$ affords a mononuclear Cu(II)−SQ species.[15]

Catechol Oxidase Activity of 2. The above results encouraged us to investigate the catechol oxidase activity of **2** using $DTBCH_2$ as a substrate. The catalytic oxidation reaction was examined by adding varied amounts of $DTBCH_2$ (0.2−5.0 mM) to the O_2-saturated acetonitrile solution of **2** (0.1 mM). The system showed an efficient catalytic activity with saturation kinetics at high $DTBCH_2$ concentrations (Figure S3).

As shown in Figure 6, the spectral changes indicate that the reaction affords an intermediate species before the formation of DTBQ. The absorptions at 313 and 750 nm, characteristic of **1**, increased in the initial stage of the reaction and then disappeared as the formation of DTBQ ceased (Figure 6B). The ESI-MS measurement confirmed the formation of **1** in the early stage of the catalytic reaction. Furthermore, with the higher concentration of $DTBCH_2$, the growth of the absorption at 750 nm became clearer (Figure S4). These results obviously demonstrate that the aerobic oxidation of $DTBCH_2$ proceeds catalytically via **1** as an intermediate.

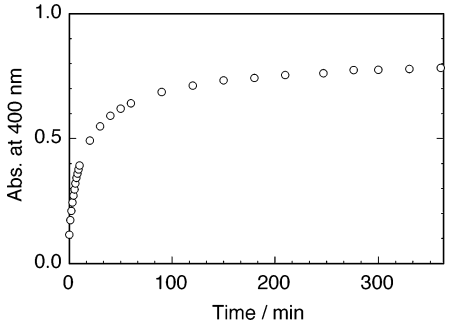

Figure 7. Time course of $DTBCH_2$ oxidation in the presence of **2** in acetonitrile. Initial concentrations: [**2**] = 48 μM, [$DTBCH_2$] = 0.77 mM, [O_2] = 0.19 mM.

It was recently reported that mononuclear Mn(III) complexes having tetradentate ligands exhibit high catechol oxidase activities.[24,25] For comparison, the initial reaction rates were analyzed by the Michaelis−Menten equation, which gave parameters of $K_m = 0.50 \pm 0.01$ mM and $k_{cat} = 336 \pm 1\ h^{-1}$. These values indicate that the present system has a slightly higher catechol oxidase activity than those reported for the mononuclear Mn(III) complexes ($K_m = 0.8-1.5$ mM and $k_{cat} = 86-230\ h^{-1}$ in methanol), provided some differences in reaction conditions are ignored.[24]

Reaction Mechanism. Many mechanistic studies on the catechol oxidase activities of copper complexes have been reported using $DTBCH_2$ as a convenient substrate.[4,7−12,14−22] In the catalytic oxidations by these complexes, dioxygen is reduced to either hydrogen peroxide in most cases[4,7−12,14,18−22] or to water in a few cases.[16,17]

$$DTBCH_2 + O_2 \rightarrow DTBQ + H_2O_2 \text{ (path A)}$$

$$DTBCH_2 + 0.5O_2 \rightarrow DTBQ + H_2O \text{ (path B)}$$

Furthermore, although Tyson and Martell reported that hydrogen peroxide is produced with *o*-quinone in catechol oxidation systems catalyzed by manganese complexes,[48] the experiment to determine the fate of the O_2 oxidant was not carried out in other manganese-catalyzed catechol oxidation systems.[24,25,49] To clarify whether dioxygen is reduced to hydrogen peroxide or water in the present system, the stoichiometry between DTBQ and the consumed dioxygen was studied by the method reported by Ackermann and coworkers.[9] The increase in the 400-nm band characteristic of DTBQ was monitored after addition of O_2-saturated acetonitrile to the N_2-saturated acetonitrile containing **2** and $DTBCH_2$ in a sealed cuvette. As shown in Figure 7, the absorbance at the end of the reaction was 0.78. Because the absorbance values were expected to be 0.40 for path A and 0.79 for path B considering the O_2 concentration (0.19 mM) in the cuvette, the above result strongly suggests path B in the present reaction. The possibility of the formation of

(48) Tyson, C. A.; Martell, A. E. *J. Am. Chem. Soc.* **1972**, *94*, 939−945.
(49) Russo, U.; Vidali, M.; Zarli, B.; Purrello, R.; Maccarrone, G. *Inorg. Chim. Acta* **1986**, *120*, L11-L13.

Scheme 2. Plausible Reaction Mechanism of the Aerobic Oxidation of $DTBCH_2$

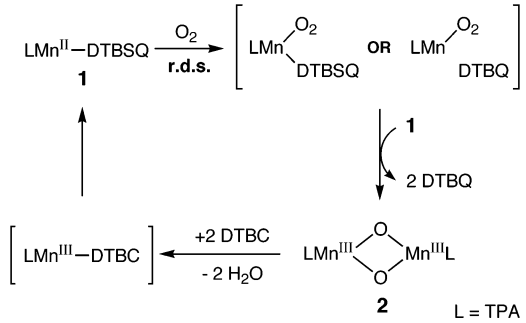

hydrogen peroxide was also excluded not only by colorimetry using a titanium(IV) sulfate complex[50] but also by the absence of bis(μ-oxo)dimanganese(III,IV) species in the reaction solution, which is formed by oxidation of **2** with H_2O_2 and results in peaks at 437, 559, and 661 nm and at 240.9 *m*/*z* ($[Mn^{III}Mn^{IV}(\mu\text{-oxo})_2(TPA)_2]^{3+}$) in the electronic absorption and ESI-MS spectra, respectively.[45,51,52]

The results obtained here suggest a mechanism depicted in Scheme 2. The conversion of **1** to **2** is initiated by dioxygen binding to the metal center of **1**, which is the rate-determining step. The resulting $Mn-O_2$ species reacts rapidly with another **1** to give the corresponding bis(μ-oxo)-dimanganese(III,III) species **2**. In these steps, dioxygen is reduced to two μ-oxo-ligands, and two DTBSQ ligands are oxidized to two DTBQ molecules. Although it is not clear at this stage what types of binuclear manganese complexes are formed in the initial stages of the formation of **2**, there may be some similarities with the formation of bis(μ-oxo)-copper(III,III) complexes in the reaction of mononuclear copper(I) complexes with O_2.[3] A similar process was reported with a mononuclear Mn(II)−thiolate complex, which reacts with dioxygen to afford the corresponding disulfide and bis-(μ-oxo)manganese(III,III) complex via a $Mn-O_2$ species as an intermediate.[53] The dinuclear complex **2** reacts with $DTBCH_2$ to give **1**, probably via a manganese(III) species $[Mn^{III}(TPA)(DTBC)]^+$ and its valence tautomerism, with the release of the μ-oxo-ligands as water molecules.

Conclusions

We demonstrated that the bis(μ-oxo)dimanganese(III,III) complex $[Mn^{III}_2(\mu\text{-oxo})_2(TPA)_2]^{2+}$ exhibits a high catechol oxidase activity. The reaction is very unique because the aerobic oxidation of catechols is catalyzed by a manganese complex via mononuclear Mn(II)−SQ and bis(μ-oxo)-dimanganese(III,III) complexes. In addition, the present system catalyzes a four-electron reduction of dioxygen to water like catechol oxidases, while most of the biomimetic complexes for catechol oxidases have been reported to produce hydrogen peroxide by a two-electron reduction of dioxygen.[4,7−12,14,18−22] Although the catechol oxidation in the present system is thought to proceed by a mechanism different from that proposed for catechol oxidases,[54] the present study no doubt contributes to the development of biomimetic complexes that can catalyze the reaction performed by catechol oxidases.

Acknowledgment. This research was supported by a Grant-in-Aid for Scientific Research (No. 14750679 to Y.H.) from the Ministry of Education, Science, Sports, and Culture, Japan and the Mizuho Foundation for the Promotion of Sciences (Y.H.). We are grateful to Prof. S. Kitagawa and Dr. H.-C. Chang for their assistance with the X-ray crystallographic analysis.

Supporting Information Available: CIF files of complexes **1** and **2**, electronic absorption spectra of **1** at 193 and 298 K and **2** at 298 K, the Michaelis−Menten plot, and time course of the absorbance changes at 400 and 750 nm in varied concentrations of $DTBCH_2$. This material is available free of charge via the Internet at http://pubs.acs.org.

IC050109D

(50) Clapp, P. A.; Evans, D. F.; Sheriff, T. S. S. *Anal. Chim. Acta* **1989**, *218*, 331−334.
(51) Suzuki, M.; Tokura, S.; Suhara, M.; Uehara, A. *Chem. Lett.* **1988**, *3*, 477−480.
(52) Gultneh, Y.; Farooq, A.; Karilin, K. D.; Liu, S.; Zubieta, J. *Inorg. Chim. Acta* **1993**, *211*, 171.
(53) Komatsuzaki, H.; Nagasu, Y.; Suzuki, K.; Shibasaki, T.; Satoh, M.; Ebina, F.; Hikichi, S.; Akita, M.; Moro-oka, Y. *J. Chem. Soc., Dalton Trans.* **1998**, 511.
(54) Solomon, E. I.; Chen, P.; Metz, M.; Lee, S.-K.; Palmer, A. E. *Angew. Chem., Int. Ed.* **2001**, *40*, 4570−4590.